Backscattering phase matrix of monodisperse ensembles of hexagonal water ice crystals

D.N. Romashov

Institute of Atmospheric Optics,
Siberian Branch of the Russian Academy of Sciences, Tomsk

Received January 12, 1999

The methodology of constructing databases for interpreting the measurements of backscattering phase matrices (BSPM) of the upper-level clouds is presented. The beam splitting method is used for calculation of the BSPM of hexagonal prisms. The influence of orientation of ice hexagonal plates and columns on the BSPM is studied. The process of formation of rays mostly contributing into the backscattering is under analysis. The BSPMs were computed for monodisperse ensembles of randomly oriented ice hexagonal plates and columns. All calculations were made for incident radiation at $\lambda = 0.55$ μm and the refractive index $m = 1.311$ (the absorption is ignored).

1. Introduction

The upper-level clouds consist principally of nonspherical water ice crystal particles having shapes of hexagonal plates and columns. At present, large bulk of data are available on the peculiarities of angular light scattering on randomly oriented water ice crystals.[1–6] Such an intent attention to this problem is caused, first of all, by an increased interest in the study of the effect of cirrus clouds on the radiation transfer through the atmosphere, as well as on the distortion of signals transmitted from onboard a spacecraft.

The problem on scattering properties of anisotropic media of water ice crystals has so far been studied too poorly, especially regarding the backscattering. The papers available from literature are based on simplified models of water ice crystals: round plates, round cylinders, and spheroids.[7–9]

An attempt is undertaken in this paper to develop a complex approach to interpretation of data of polarization lidar measurements in cirrus clouds, i.e., the methodology is described of creating databases for interpretation of polarization sounding data on the upper-level clouds.

2. Method for calculation

A lot of methods have been developed up to date for studying the light-scattering properties of water ice crystals[1–2] on the basis of the geometrical analysis of propagation of rays inside a polyhedron according to the Snell and Fresnel laws (method of ray trajectories). It is a disadvantage of some of them that the contribution of outgoing rays to the total scattered field is accepted in the form of δ-function, what, when calculating, inevitably leads to significant errors in the calculated scattering characteristics, especially for the backscattering, due to a finite grid of the scattering angles. The disadvantage of other methods is that the set of calculated scattering characteristics is incomplete. The most comprehensive approach was developed in Ref. 5, in which the method of ray trajectories is used for determining the field in the near zone on the crystal surface, and then the field in the far zone is determined on the basis of the theorem of electromagnetic equivalence. However, the use of computer codes created on the basis of this method for a personal computer is difficult due to long computation time.

The method proposed in Ref. 10 is also very promising. It considers not the rays at interaction with a polyhedron, but beams. A beam is a set of rays (equal to the point set on the plane), which were subject to identical interactions with the same sides at the output of a polyhedron (except for the external reflection). At the first interaction of a plane wave with any side, the cross section of the reflected beam is its projection on the plane perpendicular to the reflected beam direction. Analogous reasoning applies to the beam refracted inside the polyhedron after first interaction with a side. The refracted beam can be incident on several sides, i.e., the splitting of the beam occurs at the edges and vertexes. It is clear that after each internal reflection the cross sections of the beams going out of the polyhedron have a polygonal shape, and their areas decrease (except for the cases when the beam completely coincides with one of the sides). Integration over the beam cross section gives the contribution along all directions to the scattered field in the far zone. Then the fields are summed up over all outgoing beams.

Unfortunately, realization of this approach presented in Ref. 10 has some disadvantages: mathematically bulky method of ray trajectories, neglection of the diffraction contribution, the Stokes parameters of the scattered field rather than the scattering phase matrix used as output parameters.

However, because this approach allows one to save computation time, my choice is to modernize it.

When developing the program for computation of light scattering on convex polyhedrons based on the beam splitting method (BSM), the technique was used for calculating the amplitude matrices of the beam outgoing from the polyhedron,[5] as well as the algorithm for determining the boundary points of intersection of two plane polygonal areas.[10]

All other algorithms have been developed by the author. The algorithm for determining the contribution of the outgoing beam is presented in

0235-6880/99/05 376-09 $02.00

Appendix. The contribution of diffraction on the polygonal shadow of a crystal is computed in the standard way[1] with the use of the algorithm described in Appendix.

3. Backscattering phase matrix (BSPM) of a monodisperse ensemble of arbitrarily oriented hexagonal crystals

Let us set a hexagon size by means of the following parameters. Let L be the length along the symmetry axis and a be the radius of the circle circumscribed around the hexagonal base. Normally such bodies are called hexagonal columns at $L > 2a$, and hexagonal plates at $L < 2a$.

Let us describe the geometry of the scattering of radiation on an arbitrarily oriented hexagon. Let us define the coordinate system $Oxyz$ (Fig. 1) related to the incident radiation as follows: Oz axis coincides with the direction of radiation incidence, and the polarization state of the incident radiation is set relative to the xOz plane (reference plane or basis plane of the lidar). Let the coordinate system $O'x'y'z'$ be obtained from the $Oxyz$ by rotating it by three Euler angles α, β, and γ and be related to the hexagon as follows: the point O is at the center of the hexagon, Oz' axis is the symmetry axis of the hexagon, and Ox' axis is perpendicular to one of its sides.

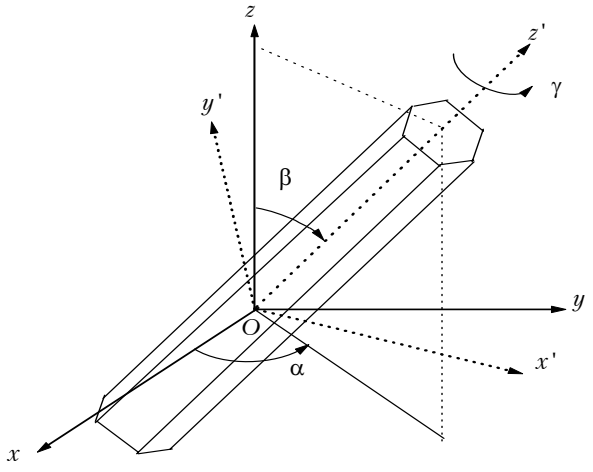

Fig. 1. Geometry of scattering on an arbitrarily oriented hexagonal crystal.

Thus, β is the angle between the radiation incidence direction and the hexagon axis, α is the angle between the reference plane and the plane containing the radiation incidence direction and the hexagon axis, and γ is the angle of rotation around the hexagon axis. We always mean averaging over this angle with the probability density $3/\pi$, i.e., if $\mathbf{S}'(\alpha, \beta, \gamma)$ is a BSPM of an arbitrarily oriented hexagonal crystal, then the BSPM averaged over the angle γ takes the form

$$\mathbf{S}(\alpha, \beta) = \frac{3}{\pi} \int_0^{\pi/3} \mathbf{S}'(\alpha, \beta, \gamma)\, d\gamma.$$

One can express $\mathbf{S}(\alpha, \beta)$ through $\mathbf{M}(0, \beta)$ (at $\alpha = 0$, the axis of hexagonal crystal lying in the reference plane) as follows:

$$\mathbf{S}(\alpha, \beta) = \mathbf{R}(-\alpha)\, \mathbf{M}(0, \beta)\, \mathbf{R}(-\alpha), \qquad (1)$$

where $\mathbf{R}(\alpha)$ is the transformation matrix of the Stokes parameters at rotation of the reference plane by the angle α:

$$\mathbf{R}(\alpha) = \begin{pmatrix} 1 & 0 & 0 & 0 \\ 0 & \cos 2\alpha & \sin 2\alpha & 0 \\ 0 & -\sin 2\alpha & \cos 2\alpha & 0 \\ 0 & 0 & 0 & 1 \end{pmatrix}.$$

To find $\mathbf{P}$, which is the BSPM of a monodisperse ensemble of hexagonal crystals polyoriented with the probability density of angular distribution $g(\alpha, \beta)$, one should integrate over the full solid angle:

$$\mathbf{P} = \int_0^{2\pi} \int_0^{\pi} \mathbf{R}(-\alpha)\, \mathbf{M}(0, \beta)\, \mathbf{R}(-\alpha)\, g(\alpha, \beta) \sin\beta\, d\beta\, d\alpha. \qquad (2)$$

Due to the symmetry of backscattering and the hexagonal crystal shape, one can take the limits of integration over α, in Eq. (2), from 0 to π and from 0 to $\pi/2$ when integrating over β.

Thus, to obtain the backscattering phase matrix of a monodisperse ensemble of arbitrarily oriented hexagonal crystals, it is necessary to calculate the matrix $\mathbf{M}(0, \beta)$ with quite a small step in the angle β and to save it as a Table (averaging over the angle γ for every fixed angle β).

Let us note that the matrix $\mathbf{M}(0, \beta)$ consists of eight non-zero elements, five of which are linearly independent,

$$M_{11}(0, \beta) - M_{22}(0, \beta) = M_{44}(0, \beta) - M_{33}(0, \beta);$$

$$M_{21}(0, \beta) = M_{12}(0, \beta); \quad M_{43}(0, \beta) = -M_{34}(0, \beta).$$

Upon accumulation of quite a large bulk of calculated data for different crystal sizes, one can calculate the backscattering phase matrix for the polydisperse ensembles of particles.

4. Calculated results

To test the program for calculating the scattering characteristics of hexagonal crystals, we have calculated elements of the scattering phase matrix (SPM) of an ensemble of randomly oriented hexagonal water ice crystals with the size $a = L = 180\ \lambda/(2\pi)$, $k = 2\pi/\lambda$ at the wavelength of the incident radiation $\lambda = 0.55$ μm and the refractive index of 1.311, while calculations of the backscattering, $\theta = \pi$, were performed by the technique described in the previous section. The calculated angular dependences of the four SPM elements: P_{22}/P_{11}, P_{33}/P_{11}, P_{44}/P_{11}, and P_{34}/P_{11},

are shown in the left panels of Fig. 2, and analogous dependences of the SPM elements calculated in Ref. 5 by the geometrical optics method of integral equations (GOM2) are shown in the right panels of Fig. 2 (solid lines). The comparison of the curves shown in Fig. 2 shows that there are small differences (about 5%) in the values of the aforementioned elements principally in the range of large scattering angles. The comparison was also carried out for the SPM elements of ensembles of randomly oriented hexagonal columns (a = 60 μm, L = 300 μm, n = 1.31, λ = 0.55 μm) and plates (a = 10 μm, L = 8 μm, n = 1.31, λ = 0.6328 μm) calculated by the author using BSM with analogous elements calculated in Ref. 2 by the method of ray trajectories (GOM1). The calculated results are presented in Table 1.

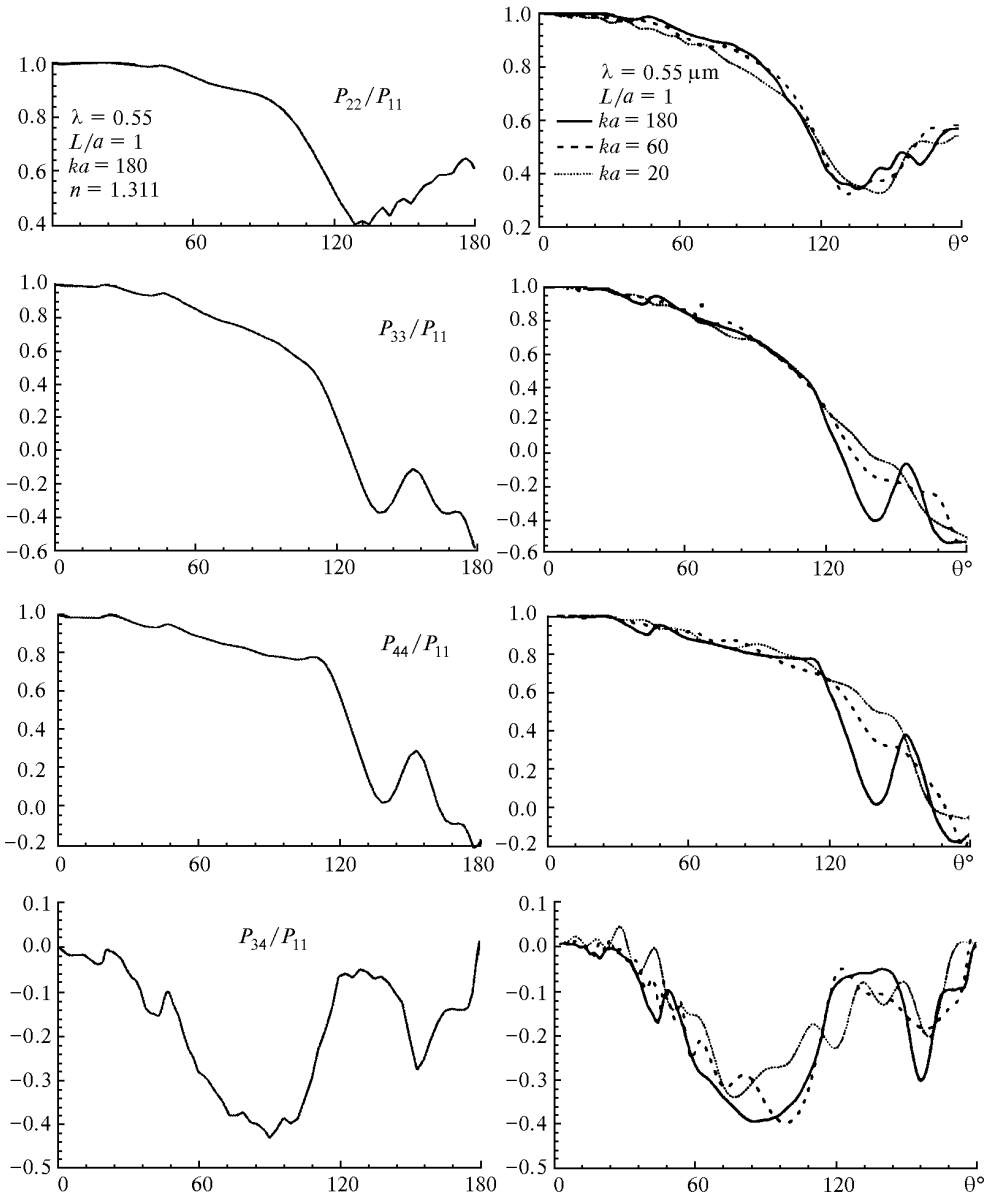

Fig. 2. The elements of the scattering phase matrix of hexagonal water ice plates randomly oriented in space. The results for backscattering are shown by dotted lines.

Table 1.

Elements of BSPM	Columns		Plates	
	BSM	GOM1 (Ref. 2)	BSM	GOM1 (Ref. 2)
P_{22}/P_{11}	0.69	0.26	0.58	0.44
P_{33}/P_{11}	–0.69	–0.26	–0.58	–0.44
P_{44}/P_{11}	–0.38	0.48	–0.16	0.12

The comparison of calculations made by the author with the analogous ones available from literature[2] shows that there are significant differences in the values of three BSPM elements ($P_{12}/P_{11} = P_{34}/P_{11} = 0$). First of all, one should note the high values of P_{44}/P_{11} and P_{33}/P_{11} and the small ones of P_{22}/P_{11} for the backscattering data presented in Ref. 2 as compared with the data calculated by the author. Let us note that the aforementioned BSPM elements calculated by BSM agree better with the experimental measurements.[11]

As mentioned above, the GOM1 method used by authors of Refs. 2 and 6 has a number of disadvantages inherent in the classical geometrical optics approach. In particular, as noted in Ref. 2, this method contains some ambiguities in calculation of the contribution to the scattered field from the beams leaving the crystal at the scattering angles $\theta = 0$ and 180° what relates to the presence of the factor $1/\sin\theta$ in the weight coefficients of the scattering amplitude for the outgoing beams. This leads to infinite scattering intensities in the forward and backward directions. To avoid this, the authors of Ref. 2 suggest to use the values $\theta = 0.5°$ and 179.5°, respectively, when calculating the weight coefficients of the beams leaving a crystal in the forward and backward directions, what should inevitably lead to large errors in the calculated values of P_{22}/P_{11}, P_{33}/P_{11}, and P_{44}/P_{11}. There is one more ambiguity of the same character, i.e., the presence of the factor $1/\sin\theta_k$ in the formula for calculating the differential scattering cross section (θ_k is the node of the grid of the polar scattering angles) in the method described in Ref. 12. Unfortunately, the authors of Ref. 5 compare the angular dependence of only two SPM elements, P_{11} and $-P_{12}/P_{11}$, calculated by the GOM1 (Refs. 1 and 2) and GOM2 (Ref. 5) methods, while it is much more interesting to compare other SPM elements. It is noted in Ref. 5 that the values P_{11} calculated for the backscattering by GOM2 are larger than the values of this element calculated by GOM1.

As numerical experiments show, the values of the elements P_{22}/P_{11}, P_{33}/P_{11}, and P_{44}/P_{11} of the BSPM of ensembles of randomly oriented hexagonal crystals at $\theta = 180°$ strongly depend on the construction of the grid of orientations over the angle α, and so one should perform calculations of the BSPM elements of randomly oriented crystals by the technique described in Section 2 (averaging over the angle α is done analytically by Eq. (2)).

Before analyzing the dependence of the BSPM $\mathbf{M}(0, \beta)$ elements introduced in Section 2, for which the averaging over the angle γ is supposed, it is interesting to study the dependence of $M_{11}'(0, \beta, \gamma)$ on the angle γ at fixed values of the angle β. Such dependence is shown in Fig. 3 for four β values. Calculations are carried out for a hexagonal water ice column with $L = 400$ μm and $a = 65.72$ μm. Let us also note that all calculations discussed in this paper have been performed for the radiation at the wavelength $\lambda = 0.55$ μm and the refractive index $n = 1.311$ (the absorption is neglected), and the relationship between a and L is calculated by the empirical formula

$$L = A(2a)^{\rho},$$

where A and ρ are the constants whose values for columns and plates can be found in Ref. 13.

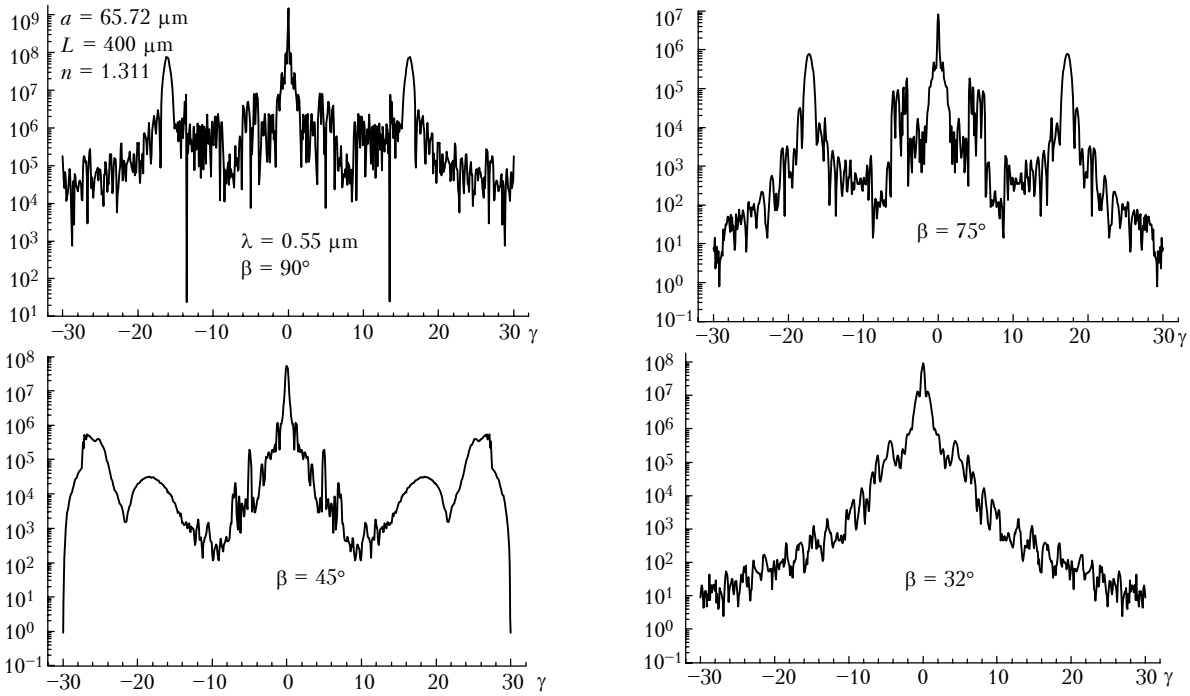

Fig. 3. The dependence of BSPM element $M_{11}'(0, \beta, \gamma)$ on the angle γ at fixed β angles: $\beta = 90$, 75, 45, and 32°.

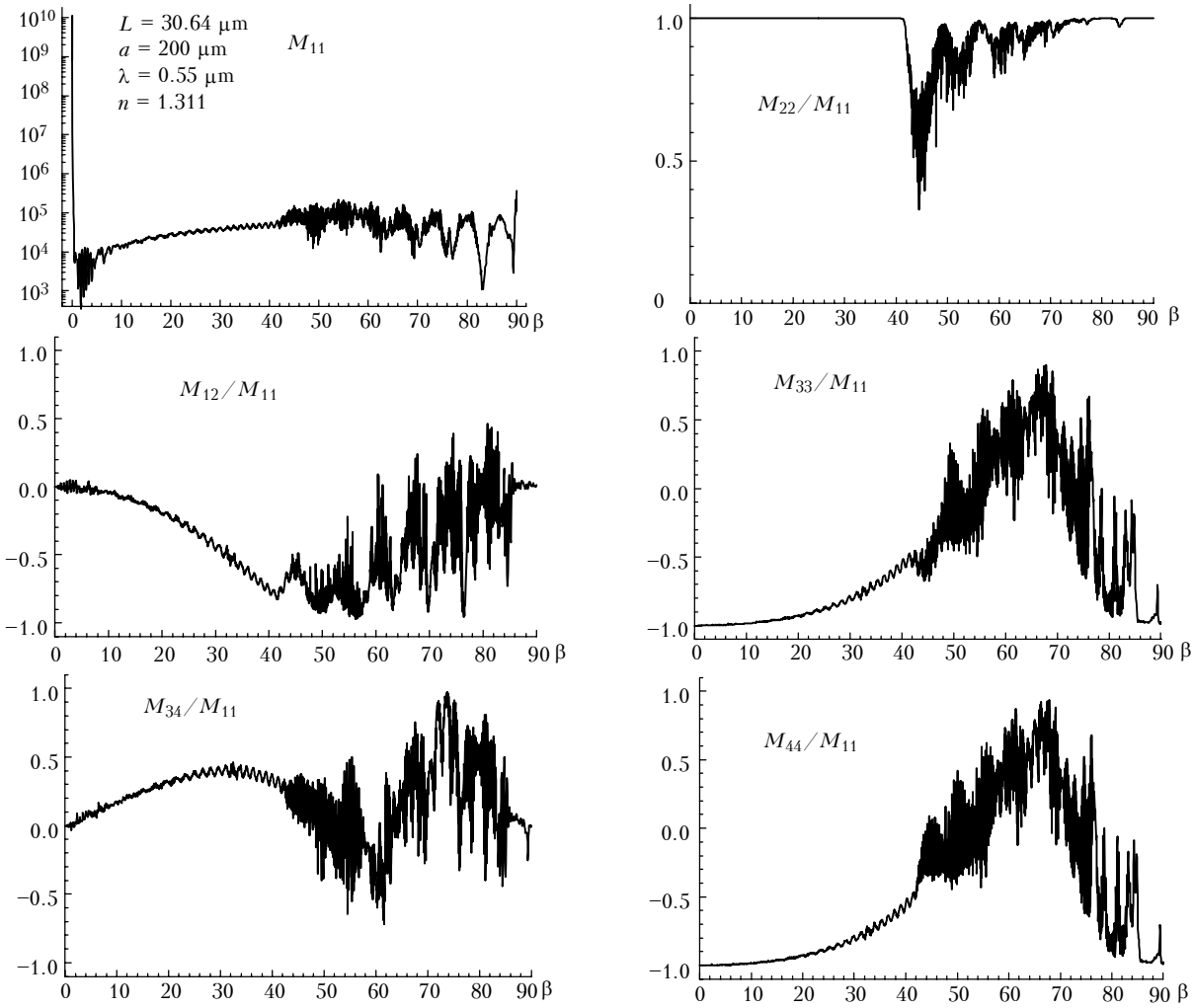

Fig. 4. The dependence of the BSPM elements on the angle β for an ensemble of hexagonal plates uniformly oriented around the axis.

As seen in Fig. 3, there is a well pronounced maximum at the point $\gamma = 0$ for all values of β. After that the values of M_{11} sharply decrease by one or two orders of magnitude as $|\gamma|$ tends to 1°. There are also quite wide, in comparison with the central peak, symmetrical side maxima, the values of which are up to 10% of the central peak value ($\gamma = 0°$), and their position on the γ axis is determined by the value of the angle β. Thus, the behavior of the BSPM, as a function of the angle β, is mainly determined by the hexagonal crystals with the orientation at $\gamma = 0°$. However, one cannot ignore the contribution of other orientations; so, it is always necessary to average, due to their rotation symmetry (of the 6th order) over the angle γ in the range $[-\pi/6, \pi/6]$ with the probability density $3/\pi$. One can estimate the contribution from particles oriented at $\gamma \neq 0°$ to the average BSPM at the fixed values β by the value of the difference $\Delta(0, \beta) = 1 - M_{22}(0, \beta)/M_{11}(0, \beta)$, because $M'_{22}(0, \beta, 0)/M'_{11}(0, \beta, 0) = 1$ at all values of β.

The angular dependences of the BSPM $\mathbf{M}(0, \beta)$ elements for a hexagonal water ice plate with the diameter $2a = 400$ μm and thickness $L = 30.64$ μm, averaged over the angle γ, are shown in Fig. 4. Averaging over the angle γ was done with the step $\Delta\gamma = 0.05°$.

As geometrical analysis of the process of formation of the beams outgoing in the backward direction, except for the values close to $\beta = 0$ and 90°, shows, the beams, for which three following conditions are satisfied, make the principal contribution to the backscatter. The conditions are:

– the beams are formed after even number of interactions with the sides (including the first external one);

– the beams go out of the same side of a crystal that has generated them at the first interaction;

– three subsequent internal interactions with the three neighboring mutually perpendicular sides necessarily take place.

Let us perform more detailed analysis of these processes by an example of hexagonal plates. Figure 5 shows the plate cross sections ($\gamma = 0°$) across its axis and the normal of two opposite tetragonal sides c_1 and c_2. The arrows show the aforementioned processes: (a) the beam goes out of the hexagonal base O_1 (Fig. 5*a*);

(b) the beam goes out of the side c_1 (Fig. 5*b*). The beams of only the 4th and 6th multiplicity of interaction are shown in Fig. 5. However, it is clear that the beams of higher even multiplicity can be formed at some values of a and L. Once changing the arrow directions in Fig. 5, we obtain the pattern of formation of mutually inverse beams which are equivalent to the initial ones in their contribution to the backscatter. The values of the cross sections of the outgoing beams are determined by the values of the parameters β, a, and L.

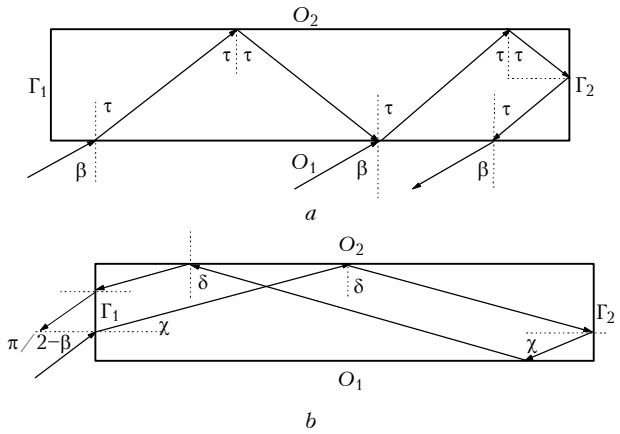

Fig. 5. Mechanisms of formation of the beams on the hexagonal plates at γ = 0°, which give the highest contribution to the backscatter at a slant incidence of radiation.

Let us analyze in a more detail the behavior of the BSPM elements as functions of the angle β for the hexagonal plates based on the aforementioned processes (γ = 0°). Let us first find the value ε, which is the angle of the total internal reflection for water ice: ε = arcsin(1/1.311) ≈ 49.7°, which takes place for the processes "a" on the side c_2 (see Fig. 5*a*) when 0° < β < 58° and processes "b" on the bases O_1 and O_2 (see Fig. 5*b*) when β > 32°. The contribution of the process "a" increases as β increases up to 58° due to the increase of the cross sections of the outgoing beams, because $L \ll 2a$, and the increase of the total internal reflection coefficient from the bases, until the total internal reflection from the side c_2 stops. The contribution of the process "b" is significant since β = 32° (the total internal reflection on the bases O_1 and O_2 appears, and the outgoing beams are formed after multiple reflections from these bases), the cross section of the beams of the fixed even multiplicity sharply increases and then decreases within a narrow range of β values, because $L \ll 2a$. The beams of higher multiplicity contribute at smaller β values, and *vice versa*. Thus, one can interpret the behavior of M_{11} in Fig. 4 as follows. The highest value of M_{11} (see Fig. 5*a*) occurs at β = 0, when $2nL = (m + 1/2)\lambda$, or at β close to 0°, when

$$2nL\,(1 - \sin^2\beta/n^2) = (m + 1/2)\lambda \qquad (3)$$

(m is an integer number). In this case the plate bases O_1 and O_2 remain practically perpendicular to the direction of radiation incidence, all reflected and multiply refracted beams go out near the forward and backward directions (in the area of the first peak of the Fraunhofer integral, see Appendix) only through the bases, and their amplitudes are summed up. It is confirmed by the behavior of $M_{11}(0, \beta)$ near β = 0 (the step is Δβ = 0.01°) for the hexagonal crystals of the length $L = 400\lambda/n$ shown in Fig. 6 where the condition (3) is satisfied at β ≈ 0.07°.

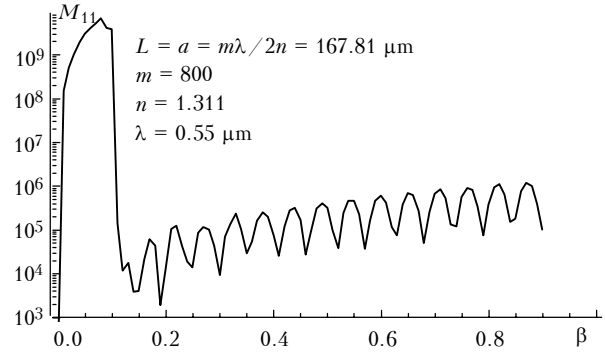

Fig. 6. The dependence of the BSPM element $M_{11}(0, \beta)$ on the angle β for a hexagonal crystal in the range from 0 to 1°.

Similar reasoning apples for β = 90°, but in this case not all refracted and reflected light beams go out in the backward direction, and the cross sections of the beams are significantly less. M_{11} monotonically increases in the range 0° < β < 42°, because the main contribution comes from the process "a". The contribution in the range 42° < β < 90° is caused by the interference of the outgoing beams resulting from the processes "a" and "b" with the prevailing contribution from the process "a" in the range 42° < β < 60° and of the process "b" in the range 60° < β < 90°. So, M_{11} periodically oscillates, first it increases and reaches maximum at the point β ≈ 58° and then decreases. The number of local maxima is determined by the ratio L/a and p that is the number of interactions to be taken into account. It equals to $p/2$ for thin plates. Up to 16 interactions were taken into account in calculations presented in Fig. 4. Let us note that the peaks near β = 0 and 90° are very narrow compared with the contribution from other orientations. In contrast to the aforementioned results, only one well pronounced maximum of M_{11} in the range 0° < β < 90° was found at β ≈ 32° when calculating BSPM of hexagonal water ice crystals, as well as two significantly lower local maxima at β = 0 and 90°.

Let us present here the qualitative analysis of the dependence of the BSPM element M_{12}/M_{11} on β (see Fig. 4). One can explain the monotonic decrease of this element to −1 as β increases from 0 to 52° by the fact that the processes of the "a" type make the principal contribution to the backscatter, and for them the total internal reflection coefficient from the plane parallel to the plane of the electric field vector incident on the bases n_1 and n_2 (see Fig. 5*a*) monotonically decreases (as β increases) and becomes equal to zero at β = 52°

(Brewster angle for water ice). Hence, the intensity of the backscattered light is maximum within the range $40° < \beta < 60°$ when it is polarized perpendicularly to the incidence plane (coinciding with the reference plane at $\alpha = 0°$). Note that one can interpret BSPM (see Fig. 4) as a BSPM at the slant sounding (zenith angle of sounding is equal to β) of an ensemble of hexagonal water ice plates, the axes of which are oriented vertically, while being uniformly distributed over the angle γ.

The behavior of M_{22}/M_{11} within the range $40° < \beta < 60°$ shows that the contribution coming from particles with the orientations at $\gamma \neq 0°$ is very significant ($M'_{22}(0, \beta, 0)/M'_{11}(0, \beta, 0) = 1$).

The dependences of the BSPM elements $\mathbf{M}(0, \beta)$ are shown in Fig. 7 for a hexagonal water ice column with the diameter $2a = 131.44$ μm and the length $L = 400$ μm. The aforementioned considerations regarding the plates apply to columns either, because in this case the bases and sides exchange their parts, and so the largest value of M_{11} occurs at the point $\beta = \pi/2$. If β_p has been one of the characteristic angles in Fig. 4, the respective angle in Fig. 6 is $\beta_c = \pi/2 - \beta_p$.

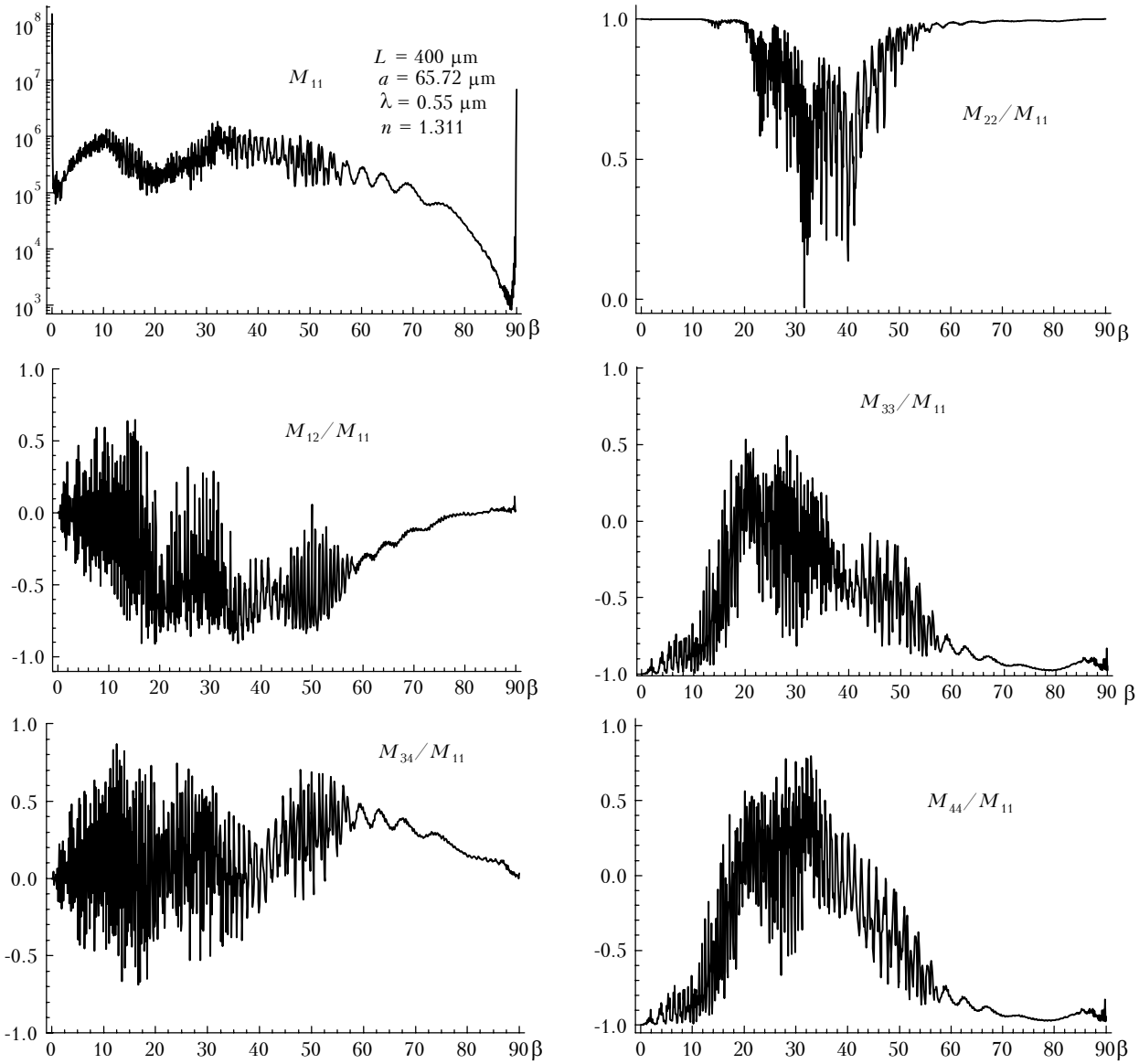

Fig. 7. The dependence of BSPM elements on the angle β for an ensemble of hexagonal columns uniformly oriented around the axis.

Let us note that there are only two local maxima of M_{11} in Fig. 7, because their quantity is determined not only by the number of interactions, which are taken into account, but also by the ratio of the maximum to minimum size of a crystal, which is significantly less for columns than for plates, calculated results for which are shown in Fig. 4.

Let us note in conclusion that the calculations carried out by the method of ray trajectories[1,2] or geometrical optics[12] cannot be satisfactory for studying

the backscatter, because they yield infinite intensity of radiation at $\theta = \pi$, and an attempt to avoid this singularity may lead to significant errors in calculating the BSPM. The method described in Ref. 7 for calculating the BSPM of round plates is free of this disadvantage, but its applicability is limited ($a \gg L$, $0° < \beta < 5°$), because it does not take into account the internal interactions with plane tetragonal sides, which make the principal contribution to the backscattering at slant orientation of crystals ($\beta \neq 0$, $\pi/2$). The aforementioned singularity (dividing by zero) is removed in the beam splitting method proposed in this paper by means of calculating the limits as it is shown in Appendix.

Appendix

Let the cross section of a polyhedron-shaped beam is determined in the coordinate system $Oxyz$ related to the incident radiation by the coordinates x_i, y_i, z_i ($i = 1, n_p$), $\mathbf{e}_p$ is the unit vector determining the direction of propagation of the beam outgoing from the crystal, $\mathbf{e}_r$ is the unit vector determining the direction of scattering, n_0 is the number of vertices of the polyhedron. Then the contribution of the beam to the resulting amplitude matrix $\mathbf{A}_p$ in the Fraunhofer diffraction approximation can be written in the form[5]:

$$\mathbf{A}_p(\mathbf{e}_r) = k^2/(4\pi)\,(1 + \mathbf{e}_r \cdot \mathbf{e}_p)\,\mathbf{S}_p\,q_p \exp(ik\delta_p), \qquad (4)$$

where $\mathbf{S}_p$ is the amplitude matrix (transformation of the amplitudes when reflecting and refracting on the sides) of the ray passing through a polyhedron vertex lying on the side from which the beam goes out, δ_0 is the phase increment of this ray,[5] and a_0 is the wave disturbance in the far zone produced by the outgoing beam calculated in the Fraunhofer diffraction approximation:

$$q_p = \iint\limits_{G_p} \exp(-ik\,\mathbf{e}_r \cdot \mathbf{r}')\,\mathrm{d}^2\mathbf{r}', \qquad (5)$$

where $k = 2\pi/\lambda$ is the wave number, λ is the radiation wavelength, G_p is the beam cross section, $\mathbf{r}'$ is the radius vector of a point in the beam cross section. As any polyhedron can be represented by a sum of triangles with respect to certain internal point O', one can rewrite Eq. (5) in the form

$$q_p = \sum_{j=1}^{n_p} q_p^j = \sum_{j=1}^{n_p} \iint\limits_{G_p^j} \exp(-ik\,\mathbf{e}_r \cdot \mathbf{r}')\,\mathrm{d}^2\mathbf{r}'. \qquad (6)$$

To make the integration in Eq. (6) easier, it is convenient to pass from the coordinate system $Oxyz$ to the coordinate system $O'x'y'z'$ related to the outgoing beam, whose axis $O'z'$ coincides with $\mathbf{e}_p$, and the point O' lies in the plane of the beam cross section inside the polyhedron. Let we have in this coordinate system that $\mathbf{e}_r = \begin{pmatrix} e_{x'} \\ e_{y'} \\ e_{z'} \end{pmatrix}$ then

$$q_p^j = \iint\limits_{G_p^j} \exp(-ik\,(e_{x'}\,x' + e_{y'}\,y'))\,\mathrm{d}x'\,\mathrm{d}y', \qquad (7)$$

where G_p^j is the triangle with the vertices $(0, 0)$, (x_j', y_j'), and (x_{j+1}', y_{j+1}'), as it is shown in Fig. 8. To calculate Eq. (7), it is necessary to make one more transformation from the coordinate system $O'x'y'z'$ to the coordinate system $O'uvz'$, i.e., the rotation around the axis $O'z'$ by the angle ϕ_j so that the axis $O'u$ passes through the point (x_j', y_j'). Numbering of the polyhedron vertices is done along the direction of positive angles in the coordinate system $O'x'y'z'$. Let us denote the coordinates of two vertices of the triangle (x_j', y_j') and (x_{j+1}', y_{j+1}') as $(u_2, 0)$ and (u_1, v_1), respectively (see Fig. 8), then we have

$$u_2 = \sqrt{x_j'^2 + y_j'^2},\ \sin\phi_j = y_j'/u_2,\ \cos\phi_j = x_j'/u_2,$$

$$u_1 = x_{j+1}'\cos\phi_j + y_{j+1}'\sin\phi_j,\ v_1 = -x_{j+1}'\sin\phi_j + y_{j+1}'\cos\phi_j;$$

$$e_u = e_{x'}\cos\phi_j + e_{y'}\sin\phi_j,\ \ e_v = -e_{x'}\sin\phi_j + e_{y'}\cos\phi_j.$$

Hence, Eq. (7) can be written in the form

$$q_p^j = \int_0^{u_1} \int_0^{\frac{v_1}{u_1}u} \exp(w_1 u + w_2 v)\,\mathrm{d}u\,\mathrm{d}v + \int_{u_1}^{u_2} \int_0^{\frac{(u_2-u)v_1}{u_2-u_1}} \exp(w_1 u + w_2 v)\,\mathrm{d}u\,\mathrm{d}v, \qquad (8)$$

where $w_1 = -ike_u$, $w_2 = -ike_v$.

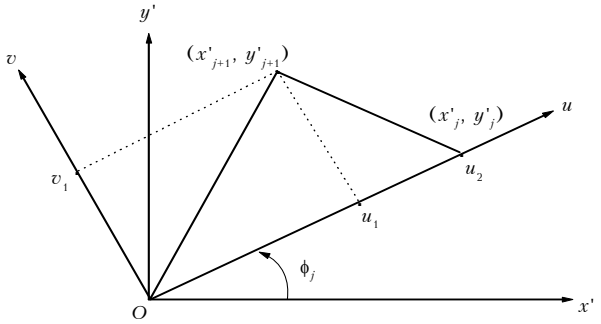

Fig. 8. Transformation of the coordinates for calculating the contribution from a triangle-shaped beam to the far zone field.

Integrating Eq. (8), we obtain

$$q_p^j = v_1 u_2\,[w_1 u_1 + w_2 v_1 - w_1 u_2 - (w_1 u_1 + w_2 v_1) \times \exp(w_1 u_2) + w_1 u_2 \exp(w_1 u_1 + w_2 v_1)]/$$

$$/[w_1 u_2\,(w_1 u_1 + w_2 v_1)\,(w_1 u_1 + w_2 v_1 - w_1 u_2)].$$

Denoting $s = w_1 u_1 + w_2 v_1$, and $d = w_1 u_2$, we finally obtain

$$q_p^j = w_1 u_2 \frac{s - d - s\,e^d + d\,e^s}{s\,d\,(s-d)}. \qquad (9)$$

To develop an algorithm for Eq. (9), it is necessary to remove the singularity of dividing by zero. There are four types of the singularity:

1) $s = 0$, $d \neq 0$; $\lim\limits_{s\to 0} \frac{s - d - s\,e^d + d\,e^s}{sd(s-d)} = \frac{e^d - d - 1}{d^2}$,

2) $d = 0$, $s \neq 0$; $\lim\limits_{d\to 0} \frac{s - d - s\,e^d + d\,e^s}{sd(s-d)} = \frac{e^s - s - 1}{s^2}$,

3) $s = d \neq 0$; $\lim\limits_{s\to d} \frac{s - d - s\,e^d + d\,e^s}{sd(s-d)} = \frac{de^d - e^d + 1}{d^2}$,

4) $s = d = 0$; $\lim\limits_{d\to 0} \frac{de^d - e^d + 1}{d^2} = \frac{1}{2}$.

The aforementioned procedure is given for an arbitrary jth triangle from a polyhedron. Applying it to all triangles of the polyhedron and summing up their contributions, we obtain the contribution coming from the entire beam.

Acknowledgments

The work was supported in part by the Russian Ministry of Science under the "LIDAR" project (No. 06–21).

References

1. Q. Cai and K.N. Liou, Appl. Opt. **21**, No. 19, 3569–3580 (1982).
2. Y. Takano and K. Jeyaweera, Appl. Opt. **24**, No. 19, 3254–3263 (1985).
3. K. Muinonen, Appl. Opt. **28**, No. 15, 3044–3050 (1989).
4. P. Yang and K.N. Liou, J. Opt. Soc. Am. A **13**, No. 10, 2072–2085 (1996).
5. P. Yang and K.N. Liou, Appl. Opt. **35**, No. 33, 6568–6584 (1996).
6. Y. Takano and K.N. Liou, Appl. Opt. **46**, No. 1, 3–19 (1989).
7. A.A. Popov and O.V. Shefer, Atm. Opt. **3**, No. 1, 36–41 (1990).
8. D.N. Romashov, Atmos. Oceanic Opt. **10**, No. 1, 4–11 (1997).
9. D.J. Wielaard, M.I. Mishchenko, A. Macke, and B.E. Carlson, Appl. Opt. **36**, No. 18, 4305–4313 (1997).
10. A.A. Popov, Izv. Vyssh. Uchebn. Zaved., Fizika, VINITI No. 8006 (1984), 56 pp.
11. B.V. Kaul', O.A. Krasnov, A.L. Kuznetsov, et al., Atmos. Oceanic Opt. **10**, No. 2, 119–125 (1997).
12. E.I. Naats, A.G. Borovoi, and U.G. Oppel, Atmos. Oceanic Opt. **11**, No. 1, 7–12 (1998).
13. O.A. Volkovitskii, L.P. Pavlov, and A.G. Petrushin, *Optical Properties of Crystal Clouds* (Gidrometeoizdat, Leningrad, 1984), 200 pp.
14. E.I. Naats, A.G. Borovoi, and U.G. Oppel, Proc. SPIE. **3583**, 155–161 (1998).